HAL
open science

Coupled Climate-Economic Modes in the Sahel's Interannual Variability

Vivien Sainte Fare Garnot, Andreas Groth, Michael Ghil

To cite this version:

Vivien Sainte Fare Garnot, Andreas Groth, Michael Ghil. Coupled Climate-Economic Modes in the Sahel's Interannual Variability. Ecological Economics, 2018, 153, pp.111-123. 10.1016/j.ecolecon.2018.07.006 . hal-01855370

HAL Id: hal-01855370

https://hal.science/hal-01855370v1

Submitted on 7 Aug 2018

HAL is a multi-disciplinary open access archive for the deposit and dissemination of scientific research documents, whether they are published or not. The documents may come from teaching and research institutions in France or abroad, or from public or private research centers.

L'archive ouverte pluridisciplinaire **HAL**, est destinée au dépôt et à la diffusion de documents scientifiques de niveau recherche, publiés ou non, émanant des établissements d'enseignement et de recherche français ou étrangers, des laboratoires publics ou privés.

The following article appeared in *Ecological Economics* **153** (2018)
and may be found at https://doi.org/10.1016/j.ecolecon.2018.07.006

Coupled climate-economic modes in the Sahel's interannual variability

Vivien Sainte Fare Garnot[a,*], Andreas Groth[b], Michael Ghil[a,b]

[a] *Geosciences Department and Laboratoire de Météorologie Dynamique (CNRS and IPSL), Ecole Normale Supérieure and PSL Research University, 24, rue Lhomond, 75005 Paris, France*

[b] *Department of Atmospheric and Oceanic Sciences, University of California at Los Angeles, Los Angeles, California, USA*

Abstract

We study the influence of interannual climate variability on the economy of several countries in the Sahel region. In the agricultural sector, we are able to identify coupled climate-economic modes that are statistically significant on interannual time scales. In particular, precipitation is a key climatic factor for agriculture in this semi-arid region. Locality and diversity characterize the Sahel's climatic and economic system, with the coupled climate-economic patterns exhibiting substantial differences from country to country. Large-scale atmospheric patterns — like the El Niño–Southern Oscillation and its quasi-biennial and quasi-quadrennial oscillatory modes — have quite limited influence on the economies, while more location-specific rainfall patterns play an important role.

Keywords: Advanced spectral methods, Business cycles, Climate cycles, Climate impacts on the economy, Sahel climate

1. Introduction

The study of climate impacts on the economy is a crucial part of assessing the stakes of ongoing global climate change. Thus, Stern (2016) called climate scientists for a closer collaboration with economists to design better models and impact assessment methods. This endeavor, though, requires one to better understand the interactions between two complex chaotic systems: the climatic and the economic one. To cope with this problem, common approaches circumvent the very difficult task of describing the internal dynamics of either system, as well as the nonlinear interactions between the two. Typically, they do so either by formulating damage functions that have little empirical basis or by applying crude regressions to historical time series.

The present work explores an alternative way based on advanced spectral decomposition methods. We focus here on the identification of endogenous dynamics in both the climatic and economic system, and the detection of coupled climate-economic behavior on interannual time scales.

To identify patterns of spatio-temporal behavior in complex datasets, we rely on multichannel singular spectrum analysis (M-SSA), which provides an efficient tool to detect and reconstruct oscillatory modes from short and noisy time series; see Ghil et al. (2002) and Alessio (2016, chapter 12) for a comprehensive overview of the methodology and of related spectral methods.

M-SSA is based on classical Karhunen (1946)-Loève (1945) theory and was introduced into the analysis of nonlinear dynamical systems by Broomhead and King (1986a,b). The methodology has found since countless applications in the geosciences (e.g., Vautard and Ghil, 1989; Ghil and Vautard, 1991) and beyond. More recently, M-SSA has been applied to study the dynamics of macroeconomic activity in the US (Groth et al., 2015) and the synchronization of business cycles, first in a set of three European countries (Sella et al., 2016) and then in more than 100 countries around the world (Groth and Ghil, 2017).

We combine here the climatic and economic system in a cross-panel M-SSA analysis to study coupled climate-economic behavior in the Sahel region. It turns out that, in this setting, M-SSA greatly helps identifying signals of interannual climate variability in the economic time series.

The Sahel's climate is very erratic and repeatedly suffered from severe droughts (Nicholson, 2013); it remains unclear whether the series of droughts has stopped now or not (Masih et al., 2014). Precipitation variability is a key climatic factor for agriculture in semi-arid regions, and thus climate change entails increased risk in such regions (Dilley, 1997). This issue, combined with the high demographic and economic stress on the region, makes it highly vulnerable and hence even more critical to investigate.

Thus, in addition to confirming the cyclic nature of climate and the economy, the paper's aim is to *determine whether climatic oscillations manifest themselves in macro-economic time series from the Sahel region.* To achieve this aim, we apply M-SSA to a dataset aggregating economic and climatic time series from the region. To

*Corresponding author
Email address:
vivien.sainte-fare-garnot@polytechnique.edu (Vivien Sainte Fare Garnot)

the best of our knowledge, such an approach has not been tried yet in the ecological economics literature, and the present paper should be read as a proof of concept.

The paper is organized as follows. In Sec. 2, we give a brief introduction to the M-SSA methodology and present a novel statistical significance test that is tailored to this paper's specific problems. Details about the dataset and the framework of the study are given in Sec. 3, while general characteristics of the time series are briefly presented in Sec. 4. In Sec. 5, we discuss the spectral properties of the combined, climatic-and-and economic dataset, while coupled climate-economic behavior is analyzed in Sec. 6. The results are discussed in Sec. 7, and the paper concludes with a summary in Sec. 8.

2. Methodology

In Sec. 2.1, we briefly describe the main steps of the M-SSA methodology, while in Sec. 2.2, the methodology for statistical-significance testing is introduced.

2.1. M-SSA

The main aspects of M-SSA are summarized here, and the reader can refer to Ghil et al. (2002) and Alessio (2016, chapter 12) for further details. A helpful illustration of the main mathematical aspects can be found in Groth and Ghil (2017).

The algorithm involves four main steps: (1) embedding, (2) decomposition, (3) rotation, and (4) reconstruction; these steps are outlined in the following.

Embedding. Consider a multivariate time series $\{x_d(n) : n = 1 \dots N; d = 1 \dots D\}$, with D channels of length N; the first step of M-SSA is to embed each channel into an M-dimensional space, where M, the window length, is a parameter. The *trajectory matrix* is thus generated by taking successive M-lagged copies from the original series:

$$\mathbf{X}_d = \begin{pmatrix} x_d(1) & x_d(2) & \cdots & x_d(M) \\ x_d(2) & x_d(3) & \cdots & x_d(M+1) \\ \vdots & & & \vdots \\ x_d(N-M+1) & \cdots & & x_d(N) \end{pmatrix} \quad (1)$$

Hence each trajectory matrix $\mathbf{X}_d$ is composed of M columns of reduced length $N' = N - M + 1$. The *augmented trajectory matrix* is then formed by concatenating all D channels,

$$\mathbf{X} = [\mathbf{X}_1, \mathbf{X}_2, \dots, \mathbf{X}_D]. \quad (2)$$

Decomposition. M-SSA then proceeds by performing a Singular Value Decomposition (SVD) of the augmented trajectory matrix,

$$\mathbf{X} = \eta^{1/2} \mathbf{P} \mathbf{\Sigma} \mathbf{E}', \quad (3)$$

where $(\cdot)'$ denotes the transpose of the argument and the normalization factor η equals $\max\{N', DM\}$. The decomposition yields a set of κ non-vanishing singular values $\{s_1, \dots, s_\kappa\}$, arranged in descending order along the main diagonal of matrix $\mathbf{\Sigma}$, with $\kappa = \min\{N', DM\}$ being the rank of $\mathbf{X}$. The matrix $\mathbf{P}$ of left-singular vectors has size $N' \times \kappa$ and provides a set of κ temporal EOFs (T-EOFs). These T-EOFs of reduced length N' reflect the corresponding behavior of an oscillation.

The matrix $\mathbf{E}$ of right-singular vectors has size $DM \times \kappa$ and provides a set of space-time empirical orthogonal functions (ST-EOFs), arranged as κ columns of length DM; it is composed of D consecutive segments $\mathbf{E}_d$ of size $M \times \kappa$,

$$\mathbf{E}' = [\mathbf{E}'_1, \mathbf{E}'_2 \dots \mathbf{E}'_D], \quad (4)$$

each of which is associated with a channel $\mathbf{X}_d$ in $\mathbf{X}$.

Combining Eqs. (2)–(4), we can easily reformulate Eq. (3) into a channel-wise notation,

$$\mathbf{X}_d = \eta^{1/2} \mathbf{P} \mathbf{\Sigma} \mathbf{E}'_d. \quad (5)$$

A helpful discussion and illustration of these mathematical properties can be found in Groth and Ghil (2017, Sec. III and Fig. 1).

Rotation. To better separate distinct oscillations, we rely here on a modified varimax rotation of the ST-EOFs, cf. Groth and Ghil (2011).

Reconstruction. The dynamical behavior of $\mathbf{X}$ associated with a subset $\mathcal{K} \subseteq \{1, \dots, \kappa\}$ of ST-EOFs can be obtained from Eq. (3) by

$$\mathbf{R}_\mathcal{K} = \eta^{1/2} \mathbf{P} \mathbf{\Sigma} \mathbf{K} \mathbf{E}'; \quad (6)$$

here $\mathbf{K}$ is a diagonal matrix of size $\kappa \times \kappa$, with the k-th diagonal element equal to one if $k \in \mathcal{K}$ and zero otherwise. Averaging along the skew diagonals of $\mathbf{R}_\mathcal{K}$, i.e., over elements that correspond in Eq. (1) to the same instant in time, finally yields the reconstructed components (RCs).

Participation index. The squares s_k^2 of the singular values equal the eigenvalue λ_k and quantify the variance in $\mathbf{X}$ that is captured by the corresponding EOF, i.e. the k-th column in $\mathbf{E}$. The contribution of channel d to this variance can be measured by the *participation index*,

$$\pi_{dk} = s_k^2 \sum_{m=1}^{M} e_{dk}^2(m), \quad (7)$$

where the sum ranges over all the elements of the k-th column in $\mathbf{E}_d$. Since the singular vectors have norm one, we get

$$\sum_{d=1}^{D} \pi_{dk} = s_k^2, \quad (8)$$

i.e. the sum of all D participation indices for a given EOF k yields the corresponding variance λ_k (Groth and Ghil, 2011).

Remark. We have followed here the original trajectory-matrix approach of Broomhead and King (1986a,b), which relies on an SVD of $\mathbf{X}$ in Eq. (3). Alternatively, one could obtain $\mathbf{E}$ from the eigendecomposition of the covariance matrix $\eta^{-1}\mathbf{X}'\mathbf{X} = \mathbf{E}\boldsymbol{\Lambda}\mathbf{E}'$ (Vautard and Ghil, 1989), with the eigenvalues $\boldsymbol{\Lambda} = \boldsymbol{\Sigma}^2$. However, in the case of a rank-deficient covariance matrix, i.e. $DM > N'$, it is more efficient to calculate the eigendecomposition from a reduced covariance matrix, $\eta^{-1}\mathbf{X}\mathbf{X}' = \mathbf{P}\boldsymbol{\Lambda}\mathbf{P}'$ (Allen and Robertson, 1996). Irrespective of the chosen algorithm, all approaches yield the same nonvanishing eigenelements (Groth and Ghil, 2015), and we use the two terms, singular values and eigenvalues, interchangeably here.

Oscillatory modes. M-SSA provides a decomposition of the dataset into distinct spectral components. The EOFs, though not purely sinusoidal, tend to have a dominant frequency that can be determined via their Fourier transform (Vautard and Ghil, 1989). It is therefore common practice to plot the eigenvalues against their corresponding dominant frequencies to obtain an estimation of the spectral decomposition of the time series.

Like the sine-cosine pairs in a Fourier analysis, the EOFs tend to pair up into oscillatory pairs (Vautard and Ghil, 1989). The two EOFs in such a pair are in phase quadrature and they capture the symmetric and antisymmetric parts of the oscillation: hence, they also have nearly equal dominant frequencies and variance levels.

The varimax rotation introduced by Groth and Ghil (2011) greatly improves the pairing of EOFs and the separation between EOFs of distinct dominant frequencies. In the absence of rotation, M-SSA is subject to a degeneracy problem and can generate spurious coupled oscillations (Feliks et al., 2013). A careful varimax-rotated M-SSA analysis will be used here in the search for coupled oscillatory modes in the climatic and economic series. Still, EOF pairing is a necessary but not sufficient criterion to determine whether or not an oscillatory component is present in the time series. Several methods have been proposed to test the statistical significance of oscillations, and the most solidly established one as yet is Monte Carlo SSA.

2.2. Significance test

Monte Carlo SSA (MC-SSA). The idea of MC-SSA is to test the statistical significance of the variance level of each eigenvalue using a Monte Carlo–type technique. The algorithm starts by fitting an autoregressive (AR) process of order 1 to each input channel of the dataset. The parameters are chosen such that this process has the same lag-0 and lag-1 covariance as the time series. An ensemble of surrogate realizations for the time series is next generated from the AR(1) process, which is then projected onto the data EOFs to derive a null-hypothesis distribution of variance levels for the significance test of the eigenvalues.

For a more complete exposition of MC-SSA see Allen and Smith (1996) and Allen and Robertson (1996), while Groth and Ghil (2015) provide a recent review of different MC-SSA techniques. A detailed application to the study of economic cycles can be found in Groth et al. (2015).

Significance test of participation index. In the original formulation of the single-channel MC-SSA significance test, the eigenvalue of a given EOF is tested against the null hypothesis of a single AR(1) process (Allen and Smith, 1996). In the multichannel case, though, a principal component analysis (PCA) is performed on the dataset prior to M-SSA, and MC-SSA is then carried out on the principal components (PCs), cf. Allen and Robertson (1996). The latter step is intended to avoid any weakening of the test against the null hypothesis of D independent AR(1) processes, due to correlations in the dataset.

The prior PCA analysis does not hinder the study of the spectral properties of the dataset, i.e. the M-SSA eigenvalues are invariant with respect to the PCA, yet the results are more abstract and harder to interpret in the PC space. The multichannel MC-SSA test will only assess whether the variance λ_k for a given EOF captured in all channels together is statistically significant.

In the present context, though, where mixed datasets of economic and climatic time series are analyzed, a modification is required as we wish to assess whether the variance of any of these channels is individually significant. A novel version of the MC-SSA methodology is therefore presented here that allows us to test the significance of the participation index π_{dk} instead.

Without any prior PCA, the algorithm starts to fit independent AR(1) processes to each of the D input channels. In the next step, an ensemble of surrogate realizations is generated, as in the standard MC-SSA test. For each surrogate realization, we form the channel-wise augmented trajectory matrix $\mathbf{X}_{R,d}$ for each input channel d as in Eq. (1) and, finally, the overall augmented trajectory matrix $\mathbf{X}_R = [\mathbf{X}_{R,1}, \cdots, \mathbf{X}_{R,D}]$, following Eq. (2).

In the classical version, due to Allen and Robertson (1996), of a multichannel MC-SSA test, the next step is to project the reduced covariance matrix $\mathbf{X}_R\mathbf{X}_R'$ onto the matrix of left-singular vectors $\mathbf{P}$,

$$\boldsymbol{\Lambda}_R = \eta^{-1}\mathbf{P}'\mathbf{X}_R\mathbf{X}_R'\mathbf{P}, \tag{9}$$

to derive the significance level for the eigenvalues, $\boldsymbol{\Lambda} = \eta^{-1}\mathbf{P}'\mathbf{X}\mathbf{X}'\mathbf{P}$, from the statistics of the diagonal elements of $\boldsymbol{\Lambda}_R$. In the terminology of Groth and Ghil (2015), this technique is referred to as unscaled target rotation onto the temporal EOFs (T-EOFs).

To understand the modifications of the significance test for the participation index, we remember that, following Eq. (2), the reduced covariance matrix of the multichannel dataset $\mathbf{X}\mathbf{X}'$ is simply the sum of D univariate covariance matrices $\mathbf{X}_d\mathbf{X}_d'$,

$$\mathbf{X}\mathbf{X}' = \sum_{d=1}^{D} \mathbf{X}_d\mathbf{X}_d'. \tag{10}$$

Note that, projecting the univariate covariance matrices onto $\mathbf{P}$ and substituting $\mathbf{X}_d'\mathbf{P} = \eta^{-1/2}\mathbf{E}_d\boldsymbol{\Sigma}$ according to

Eq. (5), we obtain

$$\eta^{-1}\mathbf{P}'\mathbf{X}_d\mathbf{X}_d'\mathbf{P} = \mathbf{\Sigma}\mathbf{E}_d'\mathbf{E}_d\mathbf{\Sigma} = \mathbf{\Pi}_d, \tag{11}$$

a diagonal matrix $\mathbf{\Pi}_d$ of size $\kappa \times \kappa$ with the k-th diagonal element equal to π_{dk}. The latter follows from the definition of π_{dk} in Eq. (7).

The modified significance test therefore proceeds, by analogy with Eq. (9), by projecting the univariate covariance matrices of the surrogate realizations onto $\mathbf{P}$,

$$\eta^{-1}\mathbf{P}'\mathbf{X}_{R,d}\mathbf{X}_{R,d}'\mathbf{P} = \mathbf{\Pi}_{R,d}, \tag{12}$$

to derive the significance level for the participation indices $\mathbf{\Pi}_d$ from the statistics of the diagonal elements of $\mathbf{\Pi}_{R,d}$.

Recall that this test on a common oscillatory mode differs from that of multiple univariate MC-SSA tests, in which the different EOF solutions are initially not linked. The observation of EOFs with similar dominant frequencies in different input channels, though, is only a necessary but not sufficient condition for the presence of coupled oscillations. It is the refined varimax M-SSA solution with the novel MC test presented herein that allows a more detailed analysis of shared mechanisms and of each channel's individual contribution to it.

Moreover, if we wish to exclude a certain part of the time series, such as the dominant trend in the economic time series, from the significance test, we follow the approach of an M-SSA composite null hypothesis (Groth and Ghil, 2015). The essential idea is to fit an AR(1) process to the RCs, as defined in Eq. (6), in which the diagonal elements of $\mathbf{K}$ equal 1 if we wish to test the corresponding EOFs and 0 otherwise.

It is important to point out that, in contrast to the common idea of first detrending the dataset prior to any spectral analysis, our single-step M-SSA analysis with its composite technique is not subject to the problem of spurious oscillations due merely to the detrending procedure itself (Nelson and Kang, 1981; Harvey and Jaeger, 1993; Cogley and Nason, 1995). Instead, our single-step M-SSA analysis provides us with a more consistent separation into a permanent trend component and transitory fluctuations that are orthogonal to it (Groth and Ghil, 2017).

3. Experimental setting

Time boundaries. In the choice of the time interval for the analysis, the limiting factor is the availability of the economic data: while climate data are available for the whole 20th century, the economic dataset chosen here is only available starting in 1960. Therefore, the time interval analyzed herein extends from 1960 to 2015. Though quite limited, this interval does have a satisfactory length for the spectral analysis of interannual variability.

The sampling interval chosen for the present study is one sample per year, which suffices to resolve periodicities of 2 years and longer. The aggregated economic series analyzed here are already provided in this form, and the climate series, though available every month, were converted into yearly time series as well. In doing so, the monthly series were first low-pass filtered with a Chebyshev type I filter to remove periodicities shorter than 2 years and then annually sub-sampled by simply taking all July values; see (Feliks et al., 2013, and the appendix therein).

Space boundaries. The Sahel represents a transitional zone, between the Sahara desert to the North and the subtropical Savannah grasslands to the South, and it thus has a semi-arid climate. When studied in a purely climatic context, the Sahel is defined as the region in which the rainfall is generally limited to the boreal summer months, with maximum rainfall occurring in August (Nicholson, 2013).

Figure 1 shows the average rainfall level in the region in January and August, corresponding to the dry and rainy season, respectively. Following Nicholson (2013), the Sahel covers the region between the latitudes of roughly 14°N and 18°N, and ranges from Sudan in the East to Senegal in the West. It includes the countries of Burkina Faso, Chad, Mali, Mauritania, Niger, Nigeria, Senegal, and Sudan[1]. The two countries Mali and Nigeria were excluded from the present study, due to a significant part of the economic data missing for the two.

Datasets. Four indicators were chosen to reflect the evolution of the economic and climatic systems of the Sahel. The gross domestic product (GDP) and agriculture value added (AVA) for the economy, and the temperature (T) and rainfall (RF) for climate. The GDP was chosen as a common aggregated measurement of economic activity, while AVA was added to study these countries' economies strong dependence on their agricultural sector. Furthermore, as agriculture in the Sahel is still mostly rainfed with little development of irrigation techniques, cf. (Rockström et al., 2009, Fig. 2.3), one can expect to see climate effects more directly in AVA than in GDP.

The two economic indicators were taken from the World Development Indicators Database[2] and the two climate indicators from the Climate Change Knowledge Portal[3]. The GDP and AVA series are both expressed in constant 2010 US$. Prior to M-SSA, the different indicators were all centered and normalized to have unit variance. Note that no prior detrending of the time series was performed to avoid problems of spurious oscillations, as already discussed in Sec. 2.2.

[1] Sudan here denotes both the recently separated countries of Sudan and South Sudan.

[2] data.worldbank.org/data-catalog/world-development-indicators

[3] sdwebx.worldbank.org/climateportal

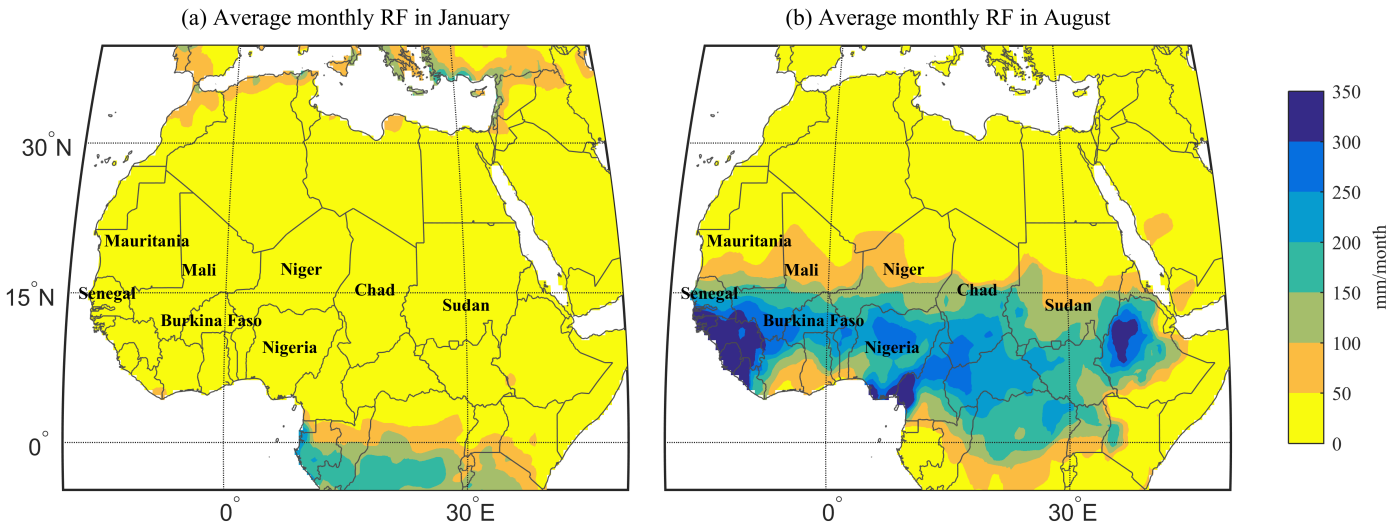

Figure 1: Average monthly rainfall in (a) January and (b) August. The average is calculated over the interval 1942–2012 from the National Oceanic and Atmospheric Administration (NOAA) PRECipitation REConstruction over Land (PREC/L) dataset (Chen et al., 2002), as given at www.esrl.noaa.gov/psd.

4. General characteristics

4.1. Climatic indicators

The climate time series are shown in Fig. 2. In the Sahel, though, rain falls during only a few summer months, so that the August peak value in Fig. 1(b), given in mm/month, is much higher than the annual value in Fig. 2(a), given in mm/year. A simple linear regression between the annual values and the peak values shows that the latter are roughly 4–6 times larger, depending on the length of the rainy season in these countries.

In the rainfall time series in Fig. 2(a), a pronounced downward trend is apparent, especially for the high rainfall rates in Burkina Faso and Senegal, from 1960 to the mid-1980s. This downward trend correlates well with the decrease in the overall Sahel precipitation index for the area (20–10°N, 20°W–10°E) (Janowiak, 1988; Becker et al., 2013), as archived at the Joint Institute for the Study of the Atmosphere and Ocean[4]. A milder increase in this index, and in the country-wise rainfall rates in our Fig. 2(a), follows from that point on to 2015.

High-amplitude year-to-year variability is superimposed on these trends, and accounts for the intense, occasionally multiannual droughts that have occurred most recently in 2010 and 2012. The droughts do not appear clearly, though, in the temperature time series that are plotted in Fig. 2(b), which mainly shows a warming trend of around 1°C over the whole time interval.

While the Sahel is often treated as one entity in the climate context, Nicholson (2013) already pointed out that notable contrasts across the region do exist. This complexity is also reflected in Fig. 2, in which the rainfall and

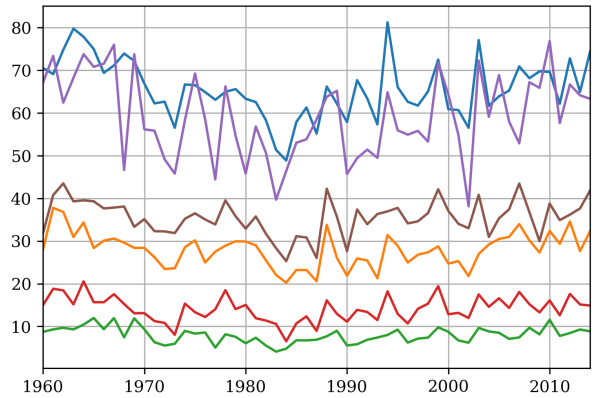

(a) Rainfall (mm/year)

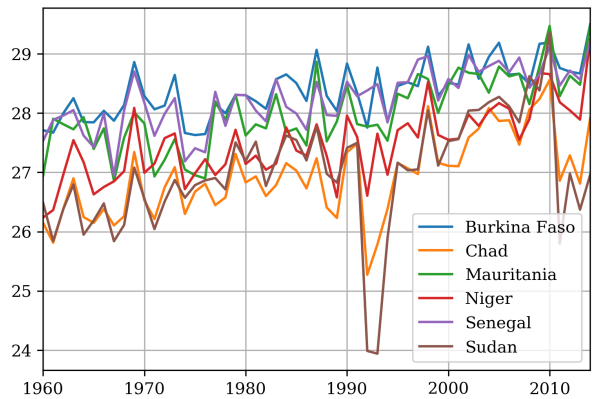

(b) Temperature (°C)

Figure 2: Climate time series of the six Sahel countries analyzed herein; see text in Sec. 3 for details of the annual sub-sampling of the monthly raw time series used here to get the plotted data.

[4] doi:10.6069/H5MW2F2Q

temperature levels do show common traits but also substantial differences.

As a consequence of the strong seasonality in the rainbelt position, we observe roughly three types of rainfall profiles in Fig. 2(a), as one crosses the Sahel from North to South:

- *Low rainfall exposure*: Countries furthest north, with only little of their territory exposed to a low level of rainfall during the rainy season. Mauritania and Niger fall into this category and have the lowest rainfall levels.

- *Intermediate rainfall exposure*: Countries extending further south, such as Chad and Sudan, with around half of their territory exposed to intermediate rainfall during the rainy season, have higher overall rainfall levels.

- *High rainfall exposure*: Countries with a significant part of their territory exposed to high intensity rainfall during the rainy season. Of the six countries considered here, Burkina Faso and Senegal fall into this category and have therefore the highest annual rainfall levels. Still, the rainfall in Senegal is more variable from year to year than in Burkina Faso. This difference is mainly due to Senegal's being closer to the northern limit of the rainbelt, whereas Burkina Faso is closer to the core. The latter is therefore less exposed to small year-to-year shifts in the rainbelt position.

4.2. Economic indicators

All six countries follow a pattern of a more or less persistent growth in GDP, with very little year-to-year variations and only a minor drop associated with the big recession of 2008 (not shown).

This GDP behavior is totally different from what we observe in the six AVA time series, shown in Fig. 3. Although persistently increasing in most of the countries, AVA is much less regular and subject to substantial variability overall, with behavior that also differs quite strikingly from country to country. Some countries, like Burkina Faso and Chad, have a more persistent trend and little year-to-year variation, while others — like Mauritania, Niger, and Senegal — have both an erratic trend and intense year-to-year fluctuations.

Generally speaking, the trend residuals of AVA capture up to 20% of the variance, while in GDP the residual variance does not exceed 2% (not shown). This pronounced variability is consistent with the lack of agricultural technologies such as irrigation in the Sahel, insofar as such technologies would tend to stabilize agricultural production (Rockström et al., 2009). Moreover, the strong year-to-year variability in AVA raises the question of potential links to climate variability on interannual time scales.

Table 1 lists the share of AVA in GDP for each of the six countries, in 1960 and 2015, respectively. In 1960, almost all economies were strongly dependent on the agricultural sector, which accounts for more than a third of GDP in the six countries, except for Senegal. In 2015, the dependency is still quite strong for most of the countries, while only Senegal and Mauritania seem to be on the way to a more industrialized economy.

Table 1: Share of AVA in GDP (in %)

Country	1960	2015
Burkina Faso	38	32
Chad	40	51
Mauritania	76	18
Niger	75	37
Senegal	24	13
Sudan	51	32

5. Spectral characteristics

We start in this section by applying M-SSA to identify oscillatory behavior in each of the two systems, climatic and economic, separately.

5.1. Economic indicators

A first set of tests was carried out on each of the two economic indicators, GDP and AVA, separately. For each of the two indicators, the six countries were combined in a single M-SSA analysis to identify cross-country relationships in the Sahel region.

The M-SSA analysis of the six AVA time series in Fig. 4 shows a rather diverse picture of distinct significant modes in each of the countries. Such diversity in the M-SSA spectra is consistent with the strong diversity already seen in the time series of Fig. 3. The diversity in the spectral characteristics apparent in Fig. 4 clearly indicates that the economic dynamics in the Sahel is less coherent than the climate dynamics and so the Sahel cannot really be considered as a single entity in the economic context. Yet, a number of significant oscillatory modes can be found in several countries.

A common oscillatory mode with a 2.4-year period is found in Burkina Faso, Chad and maybe Niger. Note that this mode is not found to be phase locked with a similar 2.4-year mode in Senegal. Moreover, a common 4.8-year mode is found in Chad, Niger, Senegal, and Sudan. Other modes appear to be more country specific, with a 4-year mode in Niger and a 3-year mode in Burkina Faso. In Mauritania, we are not able to identify any mode as statistically significant.

An equivalent M-SSA analysis was carried out on the six GDP time series (not shown), and it found similar but less numerous modes. Some of the modes we have identified in AVA are also present in the GDP spectra, a result that is consistent with the important role of the agriculture in the economy of these countries, cf. Table 1.

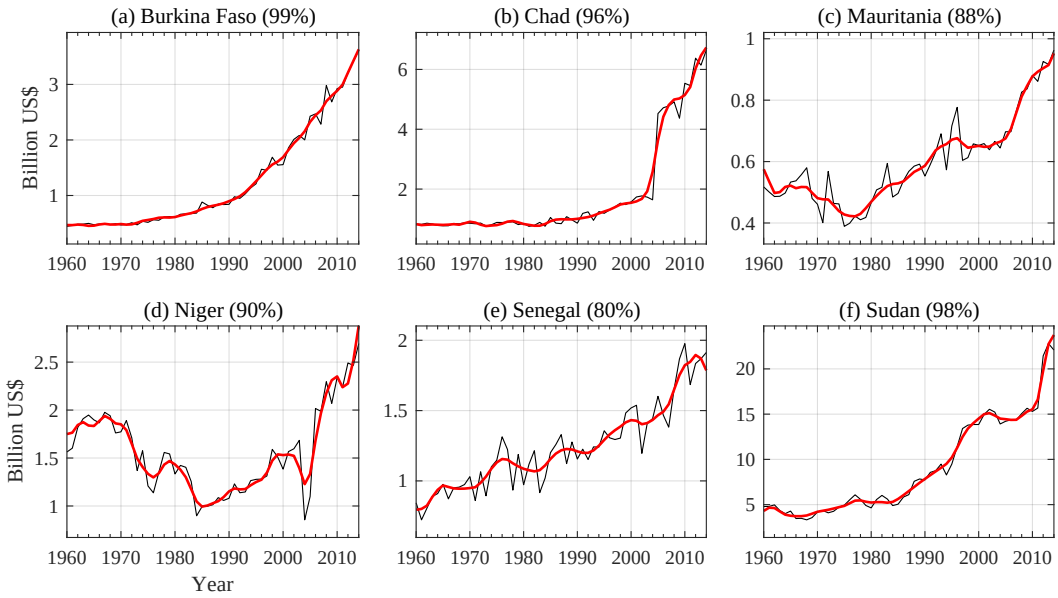

Figure 3: AVA time series (black) and estimated trend component (bold red). The trend for each country is estimated from low-frequency RCs with periods longer than 10 years, cf. Fig. 4 for additional details. The variance it captures in the AVA of each country is given in the legend of the corresponding panel (in %). Note the different scales on the y-axis.

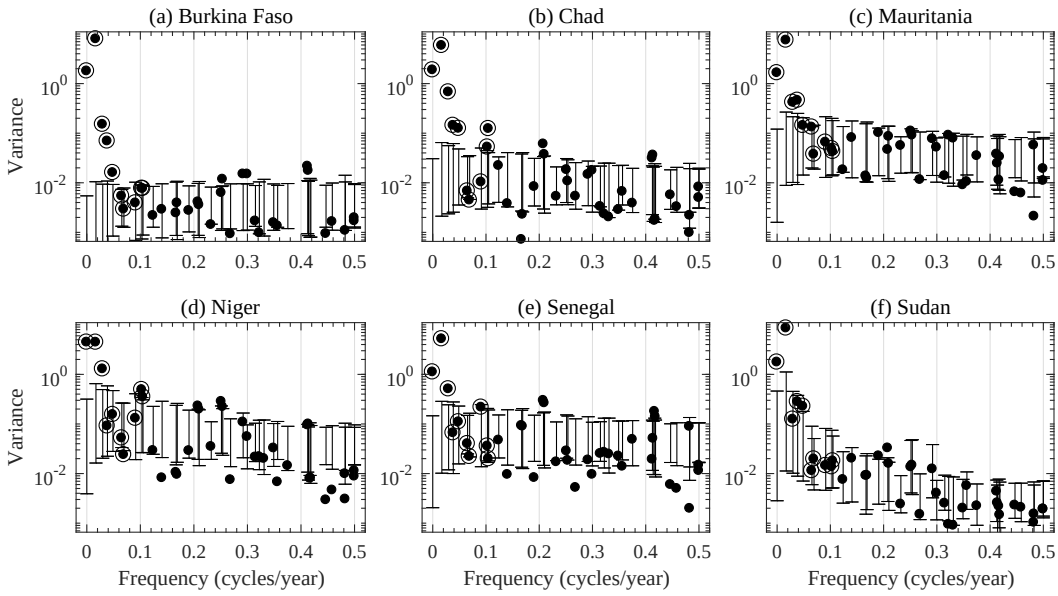

Figure 4: Cross-country M-SSA analysis of the six AVA time series from Fig. 3. The M-SSA analysis here uses a window length of $M = 18$ years; the subsequent varimax rotation uses ST-EOFs 3–40. (a–f) For each country, the variance π in each mode is shown as filled black circles, plotted as a function of the corresponding dominant frequency. Lower and upper ticks on the error bars correspond to the 2.5% and 97.5% quantiles from a Monte Carlo test of the participation index π; the test ensembles have 2500 members. In the composite null hypothesis, the low-frequency EOFs (target dots) with a period longer than 10 years are excluded from the test and the remaining EOFs are tested against AR(1) noise.

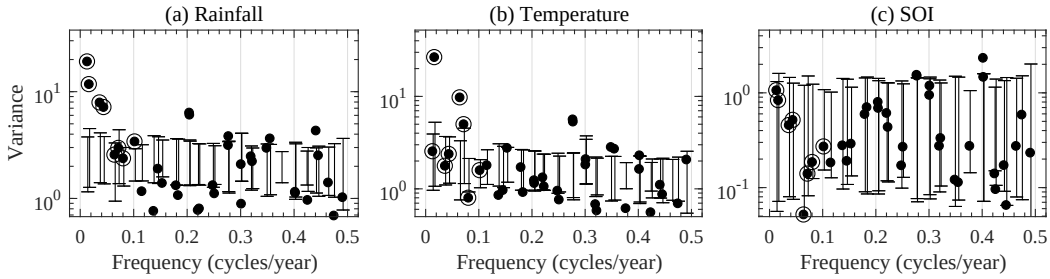

Figure 5: Cross-country M-SSA analysis of the six rainfall and six temperature time series in Fig. 2, and of the SOI index. In each mode, we plot the sum π of the of variances for (a) the six rainfall time series, and (b) the six temperature time series is shown; the significance levels are derived from a Monte Carlo test against the sum of surrogate participation indices. (c) Corresponding variance π of the SOI index. M-SSA and MC test parameters as in Fig. 4.

The variety of spectral patterns found here in the analysis of the economic indicators for the Sahel contrasts with the more synchronized behavior obtained when analyzing the economic series of developed countries within a given geographic region, such as Europe, cf. Sella et al. (2016). This finding suggests a higher diversity in the structure of the economies of developing countries within a given geographic region.

We have furthermore analyzed the possibility of coupled modes shared with several major economies. To do so, we have added the GDP time series of the US and France[5] to our M-SSA analysis, but were not able to find any of the above modes as being statistically significant in either of the two developed countries, nor were we able to find additional coupled modes at other periods.

5.2. Climatic indicators

In the spectral analysis of the climatic indicators, we have chosen to combine the rainfall and temperature time series of all six countries in a single M-SSA analysis. To include effects of other large-scale phenomena such as the El Niño–Southern Oscillation (ENSO) on the Sahel — which is known to influence the West African monsoon (Janicot et al., 1996) we have furthermore chosen to add the time series of the Southern Oscillation Index (SOI) [6] to our M-SSA analysis. The analysis presented here is only meant to give a brief idea of interannual variability in this region; a comprehensive review can be found in Nicholson (2013).

The M-SSA spectrum for the rainfall, temperature, and SOI time series is plotted in Fig. 5. In this preliminary analysis of the climate indicators, we provide only aggregated spectral properties for each of the indicators, while we leave the detailed, country-specific analysis for Sec. 6. Figures 5(a) and 5(b) thus provide only the sum of π over all rainfall and temperature time series, respectively, in each of the modes.

Comparing the spectral properties of rainfall and temperature, we observe quite a few distinct oscillations at periods similar to those in Fig. 4, while only very few modes seem to be present in both temperature and rainfall dynamics. In the spectrum of the SOI in Fig. 5(c), on the other hand, we are able to identify two modes with periods of 3.6 years and 2.4 years, respectively. These two modes agree well in their period lengths with the well-known quasi-quadrennial and quasi-biennial oscillations present in many ENSO spectra (Rasmusson and Carpenter, 1982; Jiang et al., 1995; Ghil et al., 2002), which seem therewith to affect the Sahel's rainfall and temperature fields.

6. Coupled climate-economy modes

Preliminary tests of a grand M-SSA, in which all four indicators of all six countries were combined, gave only inconclusive results (not shown). Given the diversity of spectral properties apparent in both the climate and the economic datasets, this finding is not surprising, and this approach was, therefore, discarded. A more specific, country-based analysis is adopted here instead.

After having confirmed the presence of oscillatory behavior in each indicator individually in Sec. 5, we now evaluate connections between the climate and economic indicators for each country separately. Country-based datasets were formed with the four indicators concatenated in a single M-SSA analysis, and applying the MC test procedure of Sec. 2.2 enables us to evaluate the statistical significance of each indicator's participation in coupled oscillatory modes.

The diversity of spectral characteristics that were found in each of the indicators in Sec. 5 is also reflected here in the results of the country-based analysis, and in the way the climate and economic system interact in each country. Table 2 summarizes the oscillatory modes that are significant in the country-based analysis of Burkina Faso, Niger, Senegal, and Sudan. We focus on interannual modes with periods of 2–10 years. The window length chosen here is $M = 18$ years and EOFs with periods longer than 10 years are considered to be part of the long-term trend and excluded from the significance test. Note that the results for

[5] Note that four of the six countries under consideration are subject to France's economic influence via the African Financial Community (CFA) zone.

[6] http://www.bom.gov.au/climate/current/soihtm1.shtml

Table 2: Oscillatory modes found significant in country-based M-SSA analyses. Coupled climate-economic modes in bold.

Period (in years)	GDP	AVA	RF	T
Burkina Faso				
4.8			***	
3.6				***
3.3	**	***		
2.8			**	**
2.4	*****	*****	*****	*****
Niger				
4.1		*****	*****	
3.6				***
2.8			***	**
2.2			**	
Senegal				
4.8		*****	*****	
3.6				***
3.0			**	
2.4		***		
2.3			**	
Sudan				
5.0	*****	*****		*****
4.0	**	**		
3.6			***	**
3.0			**	
2.7			**	

*** at 99% and ** at 97.5% significance level; RF = rainfall; T = temperature.

Chad and Mauritania are not included in the table, since no highly significant coupled modes were detected.

The majority of the modes are significant either in the climatic or in the economic domain, but not in both. In temperature, for example, we see a pervasive 3.6-year mode in all four countries. This mode was already detected in Fig. 5(b) and it is likely to be linked to the quasi-quadrennial ENSO oscillation, cf. Fig. 5(c); it is apparently not coupled, though, to any of the oscillatory modes of the economic time series in Table 2.

A few purely economic modes are highly significant as well. In Table 2, we see that Burkina Faso and Sudan both present oscillatory modes involving AVA and GDP, which have periods of 3.3 and 4.0 years, respectively. The rigorous application of the MC significance test shows that these modes are not merely due to the detrending of random economic fluctuations and that endogenous, deterministically generated variability has to be involved (Groth et al., 2015).

To which extent each of these endogenous modes can be attributed to adjustment delays and information lags in the market, as theorized by Kitchin (1923), is beyond the scope of the present paper. Be that as it may, both periods are consistent with the 3–4-year period of Kitchin (1923) cycles, as reviewed *in extenso* by Burns and Mitchell (1946). It appears, therefore, that some form of excitation of endogenous business cycles by a quasi-periodic climatic forcing might be at work in both countries.

Aside from the uncoupled modes in either the climatic or the economic system, we are able to identify four coupled climate-economic modes with high statistical significance, one in each country. These four are highlighted in bold in Table 2. The agricultural sector is involved in all four modes, but no other common feature can be found in all four. The details and specificities of each country are discussed in the following subsections.

Before exploring these common modes further, it is interesting to dwell on the lack thereof for two of the countries. In the case of Mauritania, this absence is consistent with the absence of significant AVA modes in Fig. 4(c). Chad, though, did exhibit two oscillatory AVA modes in Fig. 4(b); still, no evidence of climate coupling could be found here.

In neighboring Sudan, on the other hand, we do observe a 4.8-year mode in AVA, cf. Fig. 4(f); this mode is similar to the one in Chad, yet only in Sudan is a coupled oscillatory mode between AVA and temperature highly significant, as indicated in bold in Table 2.

These country-to-country discrepancies can have various causes, including the differences in their agricultural-vs.-industrial development, as per Table 1. The strong geographic diversity in the Sahel's local terrain and vegetation (Georganos et al., 2017) could also have played a role. However that may be, the example of neighboring Chad vs. Sudan shows that the occurrence of coupled climate-economic modes can be fairly localized. To which extent trade between these two countries may have led to the presence of this 4.8-year mode in Chad's AVA has to be left for future studies.

6.1. Rainfall modes in Senegal and Niger

Niger and Senegal both present a coupled mode between rainfall and agriculture, cf. Table 2, with a 4–5-year period. Figures 6(a,b) show the corresponding spectral decompositions of AVA and rainfall, respectively, from the M-SSA analysis of the four indicators for Senegal. The AVA spectrum in Fig. 6(a) is consistent with the one we have already seen in the cross-country analysis of AVA, as shown in Fig. 4(e). For Senegal, however, only the 4.8-year AVA mode is significantly coupled with rainfall, while the country's 2.4-year AVA mode is not significantly coupled with a similar but distinct 2.4-year mode in rainfall.

The reconstruction of AVA and rainfall with the RCs of the 4.8-year mode is shown in Figs. 6(c,d), respectively, together with the trend residuals; the latter are obtained by subtracting the low-frequency trend components from the raw data. In Senegal's AVA, Fig. 6(c), the 4.8-year mode captures about one third of the variance in the trend residuals and it provides a remarkably good fit to its up-and-down swings.

In Senegal's rainfall, Fig. 6(d), the 4.8-year mode captures about one quarter of the variance and it still provides a remarkably good fit to the residuals. Higher-frequency

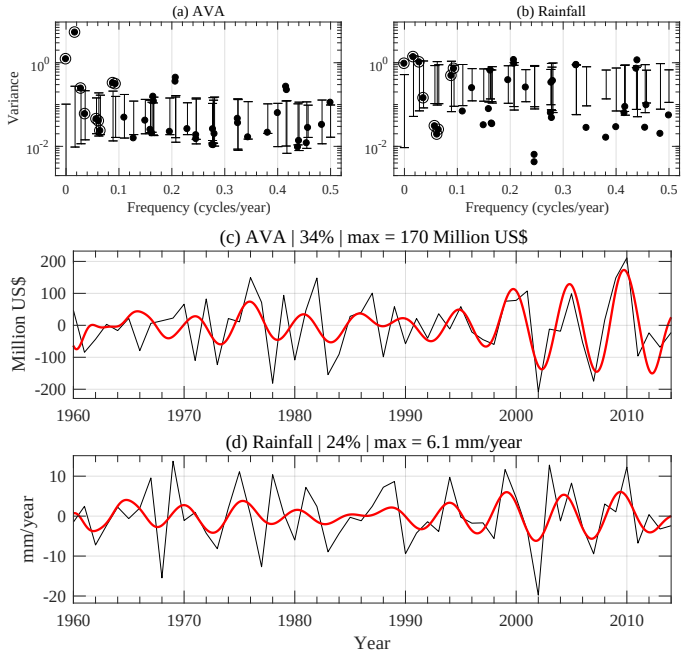

Figure 6: M-SSA analysis of the four indicators for Senegal. (a,b) Variance π of (a) AVA and (b) rainfall. (c, d) Reconstruction of the trend residuals (light black) with the RCs (heavy red) corresponding to the coupled 4.8-year mode in (c) AVA and (d) rainfall; the variance captured (in %) and the maximum values (max) are given in the legend. M-SSA and MC test parameters as in Fig. 4.

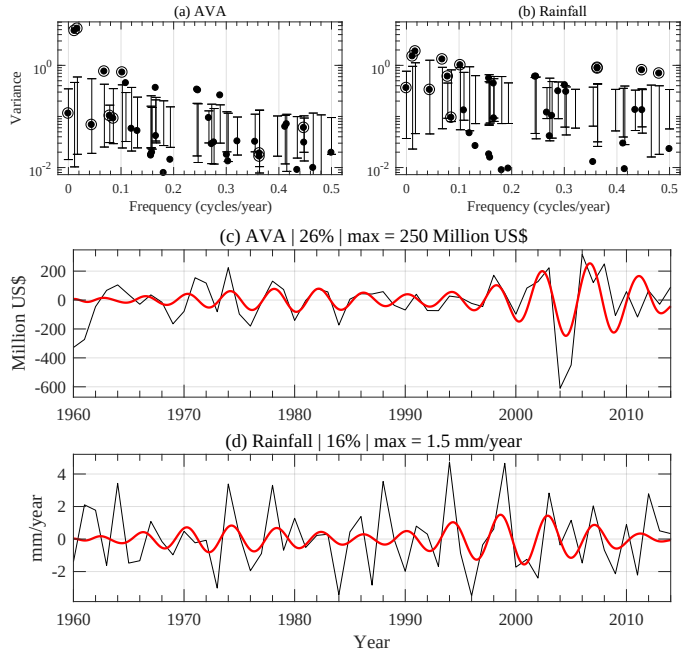

Figure 7: Same as Fig. 6, but for Niger. The reconstruction of the trend residuals (light black) in panels (c,d) uses here the RCs (heavy red) that correspond to the coupled 4.1-year mode in (c) AVA and (d) rainfall. M-SSA and MC test parameters as in Figs. 4 and 6, except two other EOF pairs, with a period of 2.8 years and 2.2 years, are excluded from the composite null hypothesis as well; see target dots in panel (a).

variations that correspond to the 2.4-year modes in AVA and rainfall, respectively, become also apparent in the trend residuals. In AVA, though, the 2.4-year mode is active during the first half of the interval only, while the 4.8-year mode begins to dominate after 1990. Although similar in their period length, M-SSA identifies the two 2.4-year modes in Figs. 6(a,b) as separate uncoupled modes, due to their different evolution in time (not shown).

The spectral decompositions of AVA and rainfall by the M-SSA analysis of the Niger dataset is shown in Figs. 7(a,b), respectively. In the composite test, we have furthermore excluded two pairs of EOFs with a period of 2.8 years and 2.2 years; these two pairs correspond to pure climate oscillations, cf. Table 2. In doing so, it turns out that we are able to identify again a coupled mode in AVA and rainfall, although with a slightly different 4.1-year period. Recall that we found both a 4.8-year and a 4.1-year mode in Niger in the cross-country analysis of AVA, as seen in Fig. 4(d); of these two, only the 4.1-year mode appears now as a coupled climate-economic mode in Fig. 7(a).

The reconstruction of AVA and rainfall with the corresponding RCs is shown in Figs. 7(c) and 7(d), respectively; the fit to the trend residuals is, once more, remarkably good in periodicity and phase, but not in amplitude: indeed, Fig. 7(b) shows that the 4.1-year mode captures only about 16% of the trend residuals' variance in rainfall, due to the presence of other significant oscillatory modes.

In both countries, the RCs of AVA and rainfall clearly suggest direct effects of rainfall variability on the AVA dynamics, while the amplitude ratio of the RCs gives an estimate of the impact. For Senegal, an approximate 6 mm/year variation in rainfall corresponds to 170 million US$ variations in AVA, cf. Figs. 6(c,d), while for Niger, an approximate 1.5 mm/year variation in rainfall corresponds to 250 million US$ variations in AVA, cf. Figs. 7(c,d). This lower sensitivity to rainfall variability in Senegal may result from differences in the exposure to rainfall, as seen in Fig. 2(a). As already discussed in Sec. 4, Senegal benefits from higher rainfall rates and it lies closer to the rainbelt core than Niger, so that small year-to-year changes in rainfall levels are more critical for Niger.

6.2. *Temperature mode in Sudan*

In contrast to the two rainfall-related modes found in Senegal and in Niger, Table 2 shows that our M-SSA analysis does not identify in Sudan a coupled climate-economic mode involving rainfall. Instead, we find a 5.0-year temperature mode, coupled to both AVA and GDP; the corresponding RCs are shown in Fig. 8. This 5.0-year mode provides a remarkably good fit to the trend residuals of AVA in Fig. 8(b), as well as to the GDP ones in Fig. 8(a). The latter fit is especially good after 1980, when the RCs reach their maximum amplitude.

Note that the RCs in temperature are anti-correlated with those of AVA and GDP, i.e. an increase in temperature has a negative effect on the economy. The amplitude ratio of the RCs suggests that an increase of approxi-

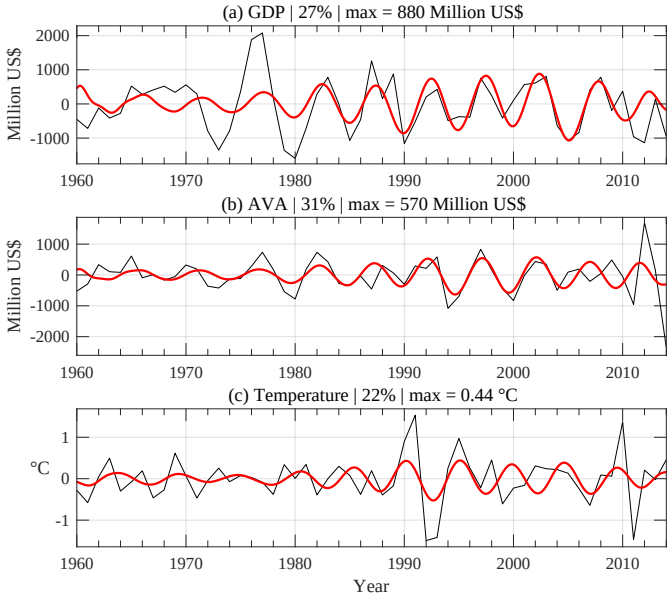

Figure 8: Trend residuals (light black) and reconstruction with the RCs (heavy red) corresponding to the coupled 5.0-year mode in Sudan; for (a) GDP, (b) AVA, and (c) temperature.

mately 0.4°C in temperature is associated with a decrease of roughly 570 million US$ in AVA and 880 million US$ in GDP.

The absence of any coupled climate-economic modes involving rainfall, though, does not necessarily mean that rainfall has no effect on Sudan's agriculture at all. We have focused here on interannual variability with 2–10-year periods, while agriculture in Sudan could be influenced by longer-term variations in rainfall, which are captured by the lowest-frequency EOFs. These low-frequency EOFs, though, have been excluded from the composite null hypothesis.

6.3. A pervasive quasi-biennial mode in Burkina Faso

In Burkina Faso, the M-SSA analysis finds a quasi-biennial 2.4-year mode to be significant in all four indicators, cf. again Table 2. The corresponding RCs are shown in Fig. 9. In AVA, this mode provides a good fit to the trend residuals and it captures 18% of the residuals' variance. In GDP, however, this mode plays only a minor role and captures no more than 3% of the variance. The RCs in the two climate indicators are anti-correlated, with higher rainfall levels and lower temperatures having a positive effect on the economy.

The amplitude ratio of the RCs suggests that an approximate 2 mm/year increase in rainfall and 0.2°C decrease in temperature correspond to an increase of roughly 110 million US$ in AVA, but only about 50 million US$ in GDP. This finding shows that Burkina Faso is less sensitive to rainfall variations in the 2.4-year coupled mode than Niger is in its 4.1-year mode, cf. Fig 7. Such a lesser sensitivity could be, once more, a result of Burkina Faso's being closer to the core of the rainbelt, so that

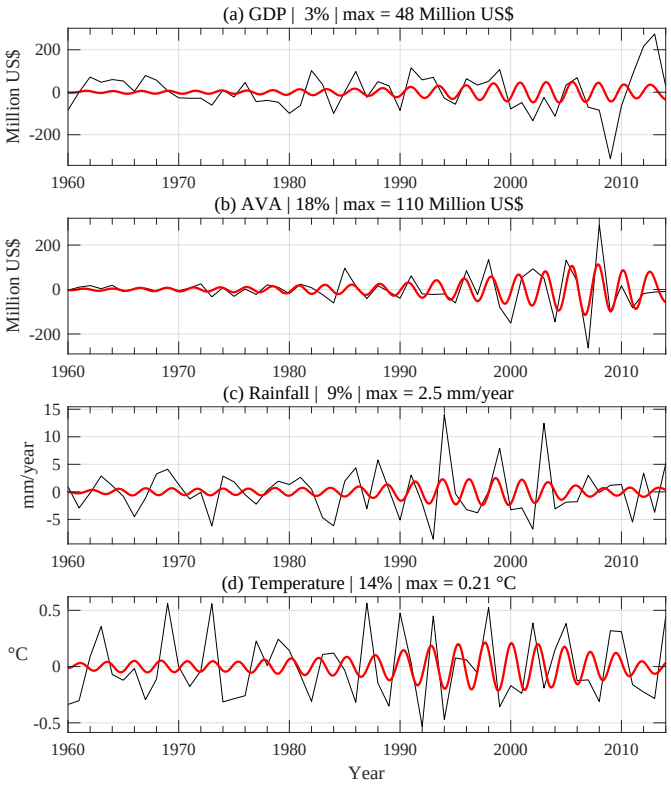

Figure 9: Trend residuals (light black) and reconstruction with the RCs (heavy red) corresponding to the coupled 2.4-year mode in Burkina Faso; for (a) GDP, (b) AVA, (c) rainfall, and (d) temperature.

year-to-year shifts are less critical for Burkina Faso than for Niger. Lastly, the higher value obtained in AVA compared to GDP is consistent with the greater volatility of agriculture observed in section 4.2.

7. Discussion

In the present study, we applied the advanced spectral M-SSA method to study the influence of climate variability on the economy, in particular the agricultural sector. Our dataset covers several economies in the Sahel region in which we are able to identify coupled climate-economic modes on interannual time scales that have high statistical significance of 97.5%–99%.

Berry and Okulicz-Kozaryn (2008) used a higher-order AR model to look for ENSO signals in the short-term fluctuations of the US economy. These authors, however, were not able to identify any co-cyclicality between ENSO and US macroeconomic indicators. Their negative result may be due to a number of causes, such as the size and complexity of the US, in which locally important climatic effects vanish; the fact that the agricultural sector accounts for as little as 1% of the US GDP in 2015; or to the lesser ability of their methodology to identify small but relatively regular effects in a sea of noisy fluctuations. On the other hand, ENSO variability has been linked to agricultural fluctua-

tions and crop yields in Mexico (Dilley, 1997), Indonesia (Naylor et al., 2001), and China (Deng et al., 2010).

In the case of the developing countries at hand, it seems that the important share of the agricultural sector, along with a low development of modern agricultural practices such as irrigation, enhances the sensitivity to climate signals in the economy. In Sec. 6, the AVA index was always involved in the coupled climate-economic modes we found to have high statistical significance. For Sudan and Burkina Faso, this climate signal was visible in GDP as well.

In the present study, we have focused on climate variability on interannual time scales, with a period of 2–10 years. Although the Sahel region is often considered as one entity, we found considerable diversity in both the Sahel's climate and economic system. It therefore happens that the coupled climate-economic modes strongly differ from country to country in their characteristics, even between neighboring countries.

We have seen, in particular, that ENSO's quasi-biennial and quasi-quadrennial oscillatory modes (Rasmusson and Carpenter, 1982; Jiang et al., 1995; Ghil et al., 2002) had only very little influence on the region's economies as a whole; see again Fig. 5(c). For Burkina Faso, though, we did identify a persistent 2.4-year mode, which could be linked to this country's geographical location and to the well-known impact of ENSO on the West African monsoon (Nicholson, 2013). For the other countries, however, a direct link to ENSO could not demonstrated by the present analysis, while large-scale climate phenomena on longer time scales might still play a role (Chang et al., 2015).

Overall, the RCs of the coupled climate-economic modes have been shown to provide a rather good reconstruction of the temporal evolution of the AVA trend residuals. The number of distinct oscillatory modes in the climate, as well as the economic system, does suggest, however, that studying climate impacts on the region's agriculture should eventually go beyond a simple linear regression.

While several climate modes were identified on interannual time scales, only a few of them appear to be coupled to the Sahel's economies. On the other hand, a few purely economic modes where identified as well and raise the question of endogenous economic dynamics and other factors outside the scope of this study.

In the present M-SSA analysis, we focused on the conceptually simplest hypothesis of a one-to-one coupling with similar periods between the climate and economic system. This restriction was chosen for the sake of simplicity, and not because the methodology is limited to the analysis of linear systems alone. Thus, for instance, Groth and Ghil (2011, 2017) found M-SSA helpful in the synchronization analysis of coupled chaotic oscillators, both in the climate and in the macroeconomics realm. Proceeding in this direction, though, will require considerable work, especially given the shortness of the available datasets.

The coupling of the two systems through a few weak oscillatory modes is interesting insofar as it is consistent with theoretical predictions about weakly coupled chaotic systems (e.g., Boccaletti et al., 2002, and references therein). In the latter, the complex behavior in each of the systems can lead to a complex synchronization process, in which weaker oscillatory modes get synchronized first (Groth and Ghil, 2011).

Finally, with respect to the assessment of climate impacts, the analysis provides some helpful insights into the sensitivity as well. The amplitude ratio in the coupled modes between the rainfall RCs and the AVA ones, for instance, provides a quantitative estimate of this sensitivity that is consistent with the country's exposure to rainfall variability. This ratio shows that Burkina Faso and Senegal, both closer to the core of the rainbelt, are less susceptible to rainfall variations, while Niger's being closer to the rainbelt's northern edge makes it more susceptible; see again Fig. 1. Although not capturing the complete, possibly nonlinear effects of rainfall on agriculture, the present analysis provides a first-order approximation of the influence of year-to-year variations in rainfall on the economy.

8. Summary

Since its introduction into the analysis of nonlinear and complex systems (Broomhead and King, 1986a,b), M-SSA has found numerous applications in the climate sciences (Ghil et al., 2002, and references therein). Recently, M-SSA has also been applied to study macroeconomic activity and global synchronization of business cycles (Groth et al., 2015; Sella et al., 2016; Groth and Ghil, 2017).

The present work goes a step further and applies the M-SSA methodology to study coupled climate-economic behavior; it also provides a novel significance test to assess whether signals of interannual climate variability can be identified in regional economic behavior. We focused on the Sahel region, including the six countries of Burkina Faso, Chad, Mauritania, Niger, Senegal, and Sudan, for which economic, as well as climatic data were available since 1960; see Secs. 1–3.

The Sahel is characterized by large variations in rainfall levels that are due to strong seasonality in the rainbelt position. The rainfall is generally limited to the boreal summer months, while small year-to-year shifts in the rainbelt position can have drastic consequences on the agricultural sector, cf. Sec. 4.

Although often considered as a single geographic entity, our results show considerable diversity in the Sahel's climatic and economic dynamics. This diversity is reflected in a number of significant oscillatory modes in each of the two systems, cf. Sec. 5.

We have chosen, therefore, to study coupled climate-economic behavior in each country individually, cf. Sec. 6. In the present analysis, we are able to identify four coupled climate-economic modes with high statistical significance, from 97.5% to 99%; see Table 2.

These four modes are present in Burkina Faso, Niger, Senegal and Sudan, and capture the temporal evolution of

the agricultural sector in these countries quite well. In Chad and Mauritania, on the other hand, the present, rather short dataset did not allow us to identify coupled climate-economic behavior. The short dataset obliged us to limit ourselves to study interannual variability with periods of 2–10 years, while longer-term climate variations (Chang et al., 2015) could still play a role.

Despite the number of distinct climate modes we found to be statistically significant in the Sahel region, it turned out that only a few of them manifest themselves as coupled climate-economic modes. In Burkina Faso, we observe a possible influence of ENSO's quasi-biennial oscillatory mode, possibly because of this country's high exposure to the West African monsoon. For the other countries, however, a direct link to ENSO is less clear from the present analysis, while connections to other large-scale climatic phenomena have to be left for future studies.

Finally, we have shown that the M-SSA analysis provides helpful insights into the sensitivity analysis of the agricultural sector with respect to year-to-year variations in rainfall, cf. Sec. 6. We showed, for example, that in Niger the sensitivity to variations in annual rainfall levels is around three times higher than in Burkina Faso and Senegal. This difference is sensitivity is likely to be due to differences in the countries' exposure to rainfall during the boreal summer months.

The wealth and variety of the present results suggests the need for refining further the application of advanced spectral methods like M-SSA to study the complex interactions between the climate and economic system. Doing so should thus help answer N. Sterns call for better methods to help the world take the road of a sounder future (Stern, 2016).

Declaration of interest

The authors have no competing interests to declare.

The present work was part of Vivien Sainte Fare Garnot's master thesis and was carried out before he joined an energy analytics company.

References

Alessio, S.M., 2016. Digital Signal Processing and Spectral Analysis for Scientists: Concepts and Applications. Springer.

Allen, M.R., Robertson, A.W., 1996. Distinguishing modulated oscillations from coloured noise in multivariate datasets. Climate Dynamics 12, 775–784. doi:doi:10.1007/s003820050142.

Allen, M.R., Smith, L.A., 1996. Monte Carlo SSA: Detecting irregular oscillations in the presence of colored noise. Journal of Climate 9, 3373–3404. doi:doi:10.1175/1520-0442(1996)009<3373:MCSDIO>2.0.CO;2.

Becker, A., Finger, P., Meyer-Christoffer, A., Rudolf, B., Schamm, K., Schneider, U., Ziese, M., 2013. A description of the global land-surface precipitation data products of the global precipitation climatology centre with sample applications including centennial (trend) analysis from 1901-present. Earth System Science Data 5, 71.

Berry, B.J.L., Okulicz-Kozaryn, A., 2008. Are there ENSO signals in the macroeconomy? Ecological Economics 64, 625–633. doi:doi:10.1016/j.ecolecon.2007.04.009.

Boccaletti, S., Kurths, J., Osipov, G., Valladares, D., Zhou, C., 2002. The synchronization of chaotic systems. Phys. Rep. 366, 1–101. doi:doi:10.1016/s0370-1573(02)00137-0.

Broomhead, D.S., King, G.P., 1986a. Extracting qualitative dynamics from experimental data. Physica D: Nonlinear Phenomena 20, 217–236. doi:doi:10.1016/0167-2789(86)90031-X.

Broomhead, D.S., King, G.P., 1986b. On the qualitative analysis of experimental dynamical systems, in: Sarkar, S. (Ed.), Nonlinear Phenomena and Chaos. Adam Hilger, Bristol, England, pp. 113–144.

Burns, A.F., Mitchell, W.C., 1946. Measuring Business Cycles. National Bureau of Economic Research, New York.

Chang, C.P., Ghil, M., Latif, M., Wallace, J.M. (Eds.), 2015. Climate Change: Multidecadal and Beyond. World Scientific Publ. Co./Imperial College Press.

Chen, M., Xie, P., Janowiak, J.E., Arkin, P.A., 2002. Global land precipitation: A 50-yr monthly analysis based on gauge observations. Journal of Hydrometeorology 3, 249–266. doi:doi:10.1175/1525-7541(2002)003<0249:glpaym>2.0.co;2.

Cogley, T., Nason, J.M., 1995. Effects of the Hodrick-Prescott filter on trend and difference stationary time series: Implications for business cycle research. Journal of Economic Dynamics and Control 19, 253–278. doi:doi:10.1016/0165-1889(93)00781-X.

Deng, X., Huang, J., Qiao, F., Naylor, R.L., Falcon, W.P., Burke, M., Rozelle, S., Battisti, D., 2010. Impacts of El Niño-Southern Oscillation events on China's rice production. Journal of Geographical Sciences 20, 3–16. doi:doi:10.1007/s11442-010-0003-6.

Dilley, M., 1997. Climatic factors affecting annual maize yields in the valley of Oaxaca, Mexico. International Journal of Climatology 17, 1549–1557. doi:doi:10.1002/(sici)1097-0088(19971130)17:14<1549::aid-joc208>3.0.co;2-n.

Feliks, Y., Groth, A., Robertson, A.W., Ghil, M., 2013. Oscillatory climate modes in the Indian Monsoon, North Atlantic and Tropical Pacific. Journal of Climate 26, 9528—9544. doi:doi:10.1175/JCLI-D-13-00105.1.

Georganos, S., Abdi, A.M., Tenenbaum, D.E., Kalogirou, S., 2017. Examining the NDVI-rainfall relationship in the semi-arid Sahel using geographically weighted regression. Journal of Arid Environments 146, 64–74.

Ghil, M., Allen, M.R., Dettinger, M.D., Ide, K., Kondrashov, D., Mann, M.E., Robertson, A.W., Saunders, A., Tian, Y., Varadi, F., 2002. Advanced spectral methods for climatic time series. Reviews of Geophysics 40. doi:doi:10.1029/2000rg000092.

Ghil, M., Vautard, R., 1991. Interdecadal oscillations and the warming trend in global temperature time series. Nature 350, 324–327.

Groth, A., Ghil, M., 2011. Multivariate singular spectrum analysis and the road to phase synchronization. Physical Review E 84, 036206. doi:doi:10.1103/physreve.84.036206.

Groth, A., Ghil, M., 2015. Monte Carlo singular spectrum analysis (SSA) revisited: Detecting oscillator clusters in multivariate datasets. Journal of Climate 28, 7873–7893. doi:doi:10.1175/JCLI-D-15-0100.1.

Groth, A., Ghil, M., 2017. Synchronization of world economic activity. Chaos: An Interdisciplinary Journal of Nonlinear Science 27, 127002. doi:doi:10.1063/1.5001820.

Groth, A., Ghil, M., Hallegatte, S., Dumas, P., 2015. The role of oscillatory modes in U.S. business cycles. OECD Journal of Business Cycle Measurement and Analysis 2015, 63–81. doi:doi:10.1787/jbcma-2015-5jrs0lv715wl.

Harvey, A.C., Jaeger, A., 1993. Detrending, stylized facts and the business cycle. Journal of Applied Econometrics 8, 231–247. URL: http://www.jstor.org/stable/2284917.

Janicot, S., Moron, V., Fontaine, B., 1996. Sahel droughts and enso dynamics. Geophysical Research Letters 23, 515–518.

Janowiak, J.E., 1988. An investigation of interannual rainfall variability in africa. Journal of Climate 1, 240–255.

Jiang, N., Neelin, J.D., Ghil, M., 1995. Quasi-quadrennial and quasi-biennial variability in the equatorial Pacific. Climate Dynamics

12, 101–112. doi:doi:10.1007/BF00223723.

Karhunen, K., 1946. Zur Spektraltheorie stochastischer Prozesse. Annales Academiæ Scientiarum Fennicæ. Ser. A1, Math. Phys. 34.

Kitchin, J., 1923. Cycles and trends in economic factors. Review of Economics and Statistics 5, 10–16. doi:doi:10.2307/1927031.

Loève, M., 1945. Fonctions aléatoires de second ordre. Comptes Rendus de l'Académie des Sciences Paris 220, 380.

Masih, I., Maskey, S., Mussá, F., Trambauer, P., 2014. A review of droughts on the African continent: a geospatial and long-term perspective. Hydrology and Earth System Sciences 18, 3635. doi:doi:10.5194/hess-18-3635-2014.

Naylor, R.L., Falcon, W.P., Rochberg, D., Wada, N., 2001. Using El Niño/Southern Oscillation climate data to predict rice production in Indonesia. Climatic Change 50, 255–265.

Nelson, C.R., Kang, H., 1981. Spurious periodicity in inappropriately detrended time series. Econometrica 49, 741–751. URL: http://www.jstor.org/stable/1911520.

Nicholson, S.E., 2013. The West African Sahel: A review of recent studies on the rainfall regime and its interannual variability. ISRN Meteorology 2013. doi:doi:10.1155/2013/453521.

Rasmusson, E.M., Carpenter, T.H., 1982. Variations in tropical sea surface temperature and surface wind fields associated with the Southern Oscillation/El Niño. Monthly Weather Review 110, 354–384. doi:doi:10.1175/1520-0493(1982)110<0354:vitsst>2.0.co;2.

Rockström, J., Karlberg, L., et al., 2009. Zooming in on the global hotspots of rainfed agriculture in water-constrained environments, in: Wani, S.P., Rockström, J., Theib, O. (Eds.), Rainfed Agriculture: Unlocking the Potential. CABI Wallingford, UK, pp. 36–43.

Sella, L., Vivaldo, G., Groth, A., Ghil, M., 2016. Economic cycles and their synchronization: A comparison of cyclic modes in three European countries. Journal of Business Cycle Research 12, 24–48. doi:doi:10.1007/s41549-016-0003-4.

Stern, N., 2016. Economics: Current climate models are grossly misleading. Nature 530, 407–409. doi:doi:10.1038/530407a.

Vautard, R., Ghil, M., 1989. Singular spectrum analysis in nonlinear dynamics, with applications to paleoclimatic time series. Physica D: Nonlinear Phenomena 35, 395–424. doi:doi:10.1016/0167-2789(89)90077-8.